Supplemental Methods

Cell culture and transfections

K562 cells were maintained as described previously[1]. We generated gCUX1 and gHPRT cell lines using the RNP-based CRISPR/Cas9 delivery system[2,3]. The BROAD shRNA Genetic Perturbation Platform (GPP) sgRNA Designer[4] was used to identify potential guides targeting *CUX1*. Potential guides were verified using the Synthego Verify Guide Design tool, and a guide targeting exon 4 of *CUX1* (5'- UGCACUGAGUAAAAGAAGCA-3') was selected. A guide targeting intron 2 of *HPRT* (5'-GCAUUUCUCAGUCCUAAACA-3') was chosen to generate an isogenic control cell line. The sgRNAs and Cas9 were obtained from Synthego. RNPs were generated by incubating the sgRNA with Cas9 at a 9:1 ratio in Buffer R for 10 minutes at room temperature. After incubation, 2 x 10^5 cells were resuspended with the Cas9-sgRNA RNPs and electroporated with 3 pulses at 1450V for 10 ms using the Neon Transfection System (ThermoFisher). Single-cell clones were generated from the transfected pool, and the clonal populations were analyzed by Sanger sequencing and western blotting. Single-cell clones with deletion of CUX1 and HPRT were used for experiments.

Western blot

K562 cells were lysed in protein lysis buffer and processed for immunoblotting as previously reported[5]. For protein detection, an antibody targeting CUX1 (B10, Santa Cruz, 1:300) followed by anti-mouse-HRP secondary antibody (Sigma, 1:5,000), and anti-β-actin-HRP (C4,Santa Cruz, 1:5,000) were used. Antibodies targeting EHMT2 (Cell Signaling, 1:1000), H3K9me1 (Sigma, 1:2000), H3K9me2 (Sigma, 1:2000), H3K9me3 (Sigma, 1:2000) and H3 (Sigma, 1:2000) were used, followed by anti-rabbit-HRP (Abcam, 1:1000).

Histone sample preparation for LC-MS/MS

Briefly, 5 x 10^6 cells were harvested 1 hour after irradiation (6 Gy) or mock irradiation, and nuclei were isolated using NEB buffer (10 mM HEPES pH 7.9, 1 mM KCl, 1.5 mM $MgCl_2$, 1mM DTT). Histones were extracted from nuclei by treatment with 0.4 N H_2SO_4 for 30 minutes at room temperature and then precipitated from the supernatant by dropwise addition of ice-cold trichloroacetic acid. Precipitated protein was spun down and washed twice with ice-cold acetone. The pellet was then air dried and resuspended in double-distilled H_2O. For each sample set, 20 µg of protein was loaded and run in a gel for 6 minutes at 200 V. Gel sections were subjected to propionyl derivatization (protein level), trypsin digestion, then propionyl

derivatization (peptide level), then C18 cleanup. For propionyl derivatization, propionic anhydride (Sigma) was mixed 1:3 with isopropanol pH 8.0 and reacted 37 °C for 15 minutes. Following protein derivatization treatment, gel sections were washed in deionized H_2O and de-stained using 100 mM NH_4HCO_3 pH 7.5 in 50% acetonitrile. A reduction step was performed by addition of 100 µl 50 mM NH_4HCO_3 pH 7.5 and 10 µl of 200 mM tris(2-carboxyethyl) phosphine HCl at 37 °C for 30 min. The proteins were alkylated by addition of 100 µl of 50 mM iodoacetamide prepared fresh in 50 mM NH_4HCO_3 pH 7.5 buffer, and allowed to react in the dark at 20 °C for 30 minutes. Gel sections were washed in water, then acetonitrile, and vacuum dried. Trypsin digestion was carried out overnight at 37 °C with 1:50-1:100 enzyme–protein ratio of sequencing grade-modified trypsin (Promega) in 50 mM NH_4HCO_3 pH 7.5, and 20 mM $CaCl_2$. Peptides were extracted with 5% formic acid and vacuum dried and sent to the Mayo Clinic Proteomics Core facility for HPLC and LC-MS/MS data acquisition. Post-digestion, peptides were derivatized with propionic anhydride:IPA 1:3 at 37 °C for 15 min and repeated for a total of two times. Peptides were then cleaned up with C18 spin columns (Pierce).

LC-MS/MS and EpiProfile analysis

Three samples of K562 gHPRT and gCUX1 irradiated (6 Gy) and mock-irradiated cells were collected one hour after treatment. Peptide samples were re-suspended in Burdick & Jackson HPLC-grade water containing 0.2% formic acid (Fluka), 0.1% TFA (Pierce), and 0.002% Zwittergent 3–16 (Calbiochem), a sulfobetaine detergent that contributes the following distinct peaks at the end of chromatograms: MH^+ at 392, and in-source dimer [2 M + H^+] at 783, and some minor impurities of Zwittergent 3-12 seen as MH^+ at 336. The peptide samples were loaded to a 0.25 µl C_8 OptiPak trapping cartridge custom-packed with Michrom Magic (Optimize Technologies) C8, washed, then switched in-line with a 20 cm by 75 µm C_{18} packed spray tip nano column packed with Michrom Magic C18AQ, for a 2-step gradient. Mobile phase A was water/acetonitrile/formic acid (98/2/0.2) and mobile phase B was acetonitrile/isopropanol/water/formic acid (80/10/10/0.2). Using a flow rate of 350 nL/minute, a 90 min, 2-step LC gradient was run from 5% B to 50% B in 60 minutes, followed by 50%–95% B over the next 10 minutes, hold 10 minutes at 95% B, back to starting conditions and re-equilibrated.

Electrospray tandem mass spectrometry (LC-MS/MS) was performed at the Mayo Clinic Proteomics Core on a Thermo Q-Exactive Orbitrap mass spectrometer, using a 70,000 RP survey scan in profile mode, m/z 340–2000 Da, with lockmasses, followed by 20 MS/MS HCD fragmentation scans at 17,500 resolution on doubly and triply charged precursors. Single

charged ions were excluded, and ions selected for MS/MS were placed on an exclusion list for 60 seconds. An inclusion list (generated with in-house software) consisting of expected histone post-translational modifications was used during the LC-MS/MS runs.

Sample *.raw files were extracted with pXtract version 2.0 to obtain their MS1 and MS2 files[6]. These along with their *.raw files were analyzed in MATLAB[7] with the EpiProfile 2.0 script[8,9]. Downstream post-translational modifications analysis was performed in Perseus version 1.6.7.0[10] and formatted in Perseus, Excel (Microsoft) or R. All code is available upon request.

ChIP-Sequencing

ChIP-seq was performed as follows. Chromatin was fixed using 1% formaldehyde for 10 minutes at RT and stopped by the addition of 0.125M glycine. Fixed chromatin was then harvested from $100x10^6$ gHPRT or gCUX1 K562 cells and sonicated (Bioruptor) for 10 minutes in 30 second on/off pulses two times for a total of 20 minutes, vortexing in between. Immunoprecipitation was performed using Dynabead protein G magnetic beads (Thermo Fischer) and 10ug of anti-H3K27Me3 (Abcam, ab6002). Following elution, samples were treated with RNAseA and proteinase K before crosslink reversal. DNA was purified using a PCR purification kit (Qiagen). Libraries were prepped using the Ovation Ultralow Library Kit (NuGEN) and size selected using with SPRIselect beads (Beckman Coulter). Illumina HiSeq was used to perform 50 bp single-end sequencing on the libraries. Two biological replicates were performed for each sample. Sequencing data are available at GEO accession number GSE154674.

ChIP-sequencing analysis

Sequencing reads were aligned to the human hg19 genome using BWA (version 0.7.12)[11] and low quality reads were removed using the SAMtools q30 filter[12]. Peaks were called using MACS2[13] with a q value threshold of 0.05. For differential peak calling, DiffBind software[14] was applied using an FDR cutoff of 0.10. The average read density from two biological replicates was normalized by RPKM in 50 bp bins and visualized using the deepTools software[15]. Statistical differences in read density were calculated using the Wilcoxon signed-rank test.

Immunofluorescence antibodies

Antibodies used for immunofluorescence in this study are as follows: γH2AX (mouse monoclonal, clone JBW301, Millipore Sigma), H3K27me3 (rabbit, monoclonal, clone C36B11, CST), H3K27me2 (rabbit, polyclonal, Sigma), H3K27me1 (rabbit, polyclonal, Sigma), H3K9me1

(rabbit, polyclonal, Sigma), H3K9me2 (rabbit, polyclonal, Sigma), H3K9me3 (rabbit, polyclonal, Sigma), EHMT2 (rabbit, monoclonal, clone C6H3, CST), phospho-ATM (mouse, monoclonal, clone 10H11.E12, CST) and 53BP1 (rabbit, polyclonal, Novus Biological). Secondary antibodies were sheep anti-mouse, Alexa Fluor 488 and goat anti-rabbit, Alexa Fluor 594 and 647.

Generation of CUX1-specific antibody: Rabbit polyclonal antibodies that recognize a C-terminal peptide amino acids 1223-1242 (CEPPSVGTEYSQGASPQPQH) of human CUX1 were generated by the Pocono Rabbit Farm and Laboratory (Canadensis, PA) and affinity purified.

Ground State Depletion (GSD) superresolution imaging

For superresolution imaging, cells were adhered to coverslips and stained as above but not mounted. Instead, coverslips were washed 5 times with PBS to remove non-specifically bound fluorophores, inverted over depression slides containing 50 µl of freshly prepared 300 mM MEA oxygen scavenging medium, sealed with a two-part, quick-curing epoxy, and cured 5 minutes in a 50° C oven. For imaging, we utilized a Leica GSD 3D imaging system equipped with a 160 X/1.43 NA, 0.07 mm WD objective; Suppressed Motion (SuMo) stage; PiFoc precision focusing control system; blue (488 nm), green (532 nm) and red (642 nm) excitation lasers; fluorescein, rhodamine and far red emission filters and an iXon Ultra EMCCD camera. Slides were then imaged using standard GSD imaging protocols with at least 10,000 frames captured per channel per image. GSD data analysis and processing were carried out with a series of custom ImageJ macros. Identification of emission events was performed via ImageJ plugin ThunderSTORM[16]. Final images were then pseudo colored and compiled in ImageJ. Superresolution imaging macros are available upon request.

GSD Fluorescence Resonance Energy Transfer (FRET) imaging

We labeled target proteins or PTMs with primary antibodies and utilized fluorescent secondary antibodies to introduce either a donor fluorophore (AF 594) or an acceptor fluorophore (AF 647). Hereafter, the labeled protein targets will be referred to as the donor and the acceptor, respectively. We first imaged both donor and acceptor at their respective excitation maxima to obtain an image of donor and acceptor location. Next, we made use of the high-powered laser on the Leica GSD microscope to deplete or bleach the acceptor fluorophores. We then imaged both donor and acceptor at their respective excitation maxima again. The second acceptor

image displayed no detectable signal indicating efficient bleaching on acceptor fluorophores. Before acceptor bleach, donor energy was transferred to the acceptor proportionately to the distance between donor and acceptor molecules. Bleached acceptor fluorophores can no longer accept donor energy, and all donor energy is thus observed when exciting donor fluorophores at donor excitation maxima. Any increase in the donor emission after acceptor bleaching is thus indicative of FRET and proportionate to the distance between acceptor and donor molecules. To obtain a FRET image, the donor image before acceptor bleach is subtracted from the donor image after acceptor bleach. The resultant image intensity is proportional to FRET between acceptor and donor. GSD-FRET reports both the location and the degree of FRET interactions between two labeled antigens. GSD-FRET imaging was carried out in the sequence described above. Images were pseudo-colored and manipulated in ImageJ.

Immunofluorescence imaging and foci analysis

For all imaging, we used round #1.5 cover glass pretreated with 0.1% poly-L-Lys for 12 hours. Coverslips were placed in 24-well plates and approximately 250,000 K562 cells were seeded into each well and allowed to grow for 12-24 hours. Irradiation and/or treatment with indicated inhibitors were performed *in situ*. For slide preparation, plates were spun in a benchtop centrifuge at 500 G for 5 minutes to aid in cell adhesion. Subsequently, cells were fixed with 4% PFA in PBS for 10 minutes at the indicated time point, stained with 0.5 µg/mL DAPI, and mounted using ProLong Gold (Invitrogen). For immunofluorescence staining, cells were fixed as above, then permeabilized with 10% Triton-X 100 for 10 minutes. After blocking with 5% BSA in PBS for 1 hour, the indicated primary antibodies were added and coverslips were incubated overnight at 4°C. All antibodies were used at 1:1000 dilution. Following three 5 minute washes with 5% BSA in PBS supplemented with 0.1% TX-100 and 0.05% NP-40, fluorescent secondary antibodies (Jackson ImmunoResearch) were applied for 1 h at room temperature. All images were captured on an Olympus IX81 wide-field microscope with either 150X oil-immersion objective and pseudo colored using ImageJ. 2-3 biological replicates were performed (as indicated in the legend) for each experiment and greater than 50 cells were imaged per replicate. Foci counting was performed with a custom ImageJ macro. Briefly, nuclei were thresholded and segmented and foci were counted within each nucleus via a thresholding and FindMaxima routine. Foci intensity analysis was performed by segmenting the foci as above and then measuring the MFI within each focus. Foci within each nucleus were grouped, and the mean Foci-MFI value was reported per nucleus. Foci size was determined by auto-local thresholding of the γH2AX channel followed by segmentation and measurement of segmented

foci regions. All other image analysis was carried out in ImageJ via custom macros. All macros available upon request.

Mouse models

All animal studies were approved by the University of Chicago Institutional Animal Care and Use Committee mice were housed in Association for Assessment and Accreditation of Laboratory Animal Care-accredited, specific pathogen-free animal care facilities at the University of Chicago. Both sexes of mice were used, and experimental mice were housed separately by sex with five mice per cage. Tail clips were performed for genotyping. Renilla, shCux1.581 ($Cux1^{mid}$) and shCux1.2812 ($Cux1^{low}$) mice were generated as previously described[5]. A second-generation reverse tet-transactivator (M2rtTA) is expressed from the endogenous *ROSA26* promoter, and an shRNA targeting Renilla luciferase or *Cux1* is expressed downstream of *Col1a1.* Resulting mice were rtTA-$M2^{tg/tg}$;$Col1a1^{Cux1/wt}$ (either $Cux1^{low}$ or $Cux1^{mid}$) or rtTA-$M2^{tg/tg}$;$Col1a1^{Ren/wt}$ (Ren) littermate controls, on a mixed C57BL/6 x 129/Sv background. The transgene was induced by maintaining the mice on continuous doxycycline-containing chow diet (TD.12006, 1 mg/kg, Envigo). For all experiments, adult mice (8-16 weeks) were used. ENU (Sigma) was administered intraperitoneally at 100 mg/kg at the times indicated in the legend.

Flow Cytometry

Peripheral blood was collected from the submandibular vein for complete blood counts and flow cytometry. Complete blood counts were performed using a Hemavet 950 counter (CDC Technologies, Oxford, CT). For flow cytometry, 50 uL of blood was blocked with an Fc receptor blocking reagent (clone 93, Fisher Scientific), split into two aliquots and stained with CD45-BUV395 (30-F11, Fisher Scientific) and either CD3e-APC (145-2C11, BD Biosciences) and B220-PE (RA3-6B2, eBioscience), or Gr1-PE (RB6-8C5, Fisher Scientific) and CD11b-APC (M1/70, BD Biosciences). For competitive transplants and autopsy analysis, the peripheral blood, BM and spleen were stained with the following antibodies (BD Biosciences): PerCP-Cy5.5-CD45R/B220 (RA3-6B2), BUV737-CD3e (145-2C11), BUV395-Gr1 (1A8), APC-Cy7-CD11b (M1/70), PE-CD45.1 (A20), APC-CD45.2 (104). Cells were incubated for 30 minutes at room temperature and then lysed with ACK red blood cell lysis buffer prior to analysis.

For BM and spleen analysis, cells were lysed by ACK lysis buffer, FcR blocked and stained with the following biotin-conjugated lineage markers (BD Biosciences): CD3e (145-2C11), CD5 (53-7.3), CD19 (1D3), CD11b (M1/70), Gr-1 (RB6-8C5), Ter119 (Ter-119), and B220 (RA3-6B2) for 20 minutes on ice. For stem cell analysis, cells were washed with flow

buffer and stained with the following (BD Biosciences): cKit-APC-Cy7 (2B8), Sca-1-PE-Cy7 (D7), Streptavidin-BUV737, CD45.1-BUV395 (A20), CD45.2-APC (104), CD48-Percp/Cy5.5 (HM48-1), CD150-PE (Q38-480). For myeloid progenitor cells, the following antibodies were used: cKit-APC-Cy7 (2B8, BD Biosciences), Sca-1-PE-Cy7 (D7, BD Biosciences), CD45.2-BUV737 (104, BD Biosciences), Streptavidin-BUV395 (BD Biosciences), CD34-eFluor-660 (RAM34, Invitrogen/eBioscience), CD16/32-PerCP-5/Cy5.5 (2.4G2, BD Biosciences), CD45.1-PE (A20, BD Biosciences). Cells were incubated for 30 minutes at room temperature. Staining for γH2AX, BrdU and cPARP were performed according to the manufacturer protocol (BD Biosciences, 562253). Flow cytometry was performed on an LSR Fortessa (BD Biosciences), and data analyzed with FlowJo software (Tree Star, Inc., Ashland, OR).

For erythroblast analysis of the spleen and bone marrow, cells were FcR blocked and stained with the following antibodies from Fisher Scientific: Ter119-PE (Ter-119), and CD71-APC (C2). For Ter119 and CD71 erythroblast analysis, cells were analyzed without red cell lysis.

RNA-seq

Adult Ren and Cux1^{low} mice were treated with doxycycline for 5 days, and bone marrow cells were collected and lysed. BM cells were lineage depleted (Mouse Direct Lineage Cell Depletion kit, Miltenyi Biotec) and stained. HSCs (Lin$^-$, cKit$^+$, Sca1$^+$, CD135$^-$) were sorted on a FACSAria II (BD Biosciences) directly into Trizol. RNA was purified by RNeasy Kit (Qiagen), and >100 ng of RNA was used for library preparation. Three biological replicates were performed.

Barcoded RNA-seq libraries were generated with the TruSeq v2 kit (Illumina) and >23 million, single end, 50 bp reads were generated by Illumina sequencing (HiSeq 2000). Reads were aligned using STAR[17], and alignments with a mapping quality <30 were removed. Differential gene expression analysis was performed using DESeq2[18], and a negative binomial general linearized model fitting and Wald statistics were used to generate p values, with p values adjusted using the Benjamini Hochberg method. Sequencing data are available in the GEO Database (accession GSE154674).

γH2AX Assay

Mice were treated with dox for 7 days, and bone marrow was collected. Whole bone marrow was cultured overnight in StemSpan SFEM medium (Stemcell Technologies) supplemented with β-mercaptoethanol (55 uM), doxycycline (1 μg/mL), murine stem cell factor (100 ng/mL), murine

IL-3 (100 ng/mL), murine IL-6 (100 ng/mL) and FBS (10%) prior to treatments. Bone marrow was irradiated (2 Gy) or mock-irradiated, and cells were collected at the time points indicated. Lineage-negative cells and $Lin^-/cKit^+/Sca1^+$ (LSK) cells were gated.

Proliferation and Apoptosis assays

K562 cells were irradiated (6 Gy) and cultured for 24 hours. One hour before collection, BrdU was added to the culture for a final concentration of 10 μM. For *in vivo* experiments, mice were given continuous doxycycline for one week before injecting ENU (100 mg/kg) intraperitoneally (IP). A second dose of ENU was administered 9 days later, and BrdU was injected IP 6 hours after ENU. BM and spleen cells were collected 12 hours after BrdU. Murine cells were then stained for stem cell and progenitor markers, and BrdU and cPARP staining were performed according to the manufacturers protocol (BD Biosciences, 562253).

Histology

Tissues were fixed in 10% formalin, embedded in paraffin, sectioned at 4 μm, and stained with hematoxylin and eosin or GATA1. Images were taken with a Zeiss Axioskop microscope.

Comet single cell electrophoresis assay

Ren, $Cux1^{mid}$ and $Cux1^{low}$ mice were treated with doxycycline for 7 days and irradiated (6 Gy). Bone marrow cells were collected at the indicated times following irradiation, and $cKit^+$ cells were selected (Mouse CD117 Microbead kit, Miltenyi Biotec). Cells were embedded in low-melting agarose (Trevigen). Comet assays were performed with a Trevigen Comet Kit according to manufacturer's directions with the following modifications. Cells were electrophoresed at 23 V for 60 min and stained with SYBR Green rather than SYBR Gold. Imaging of comet slides was carried out on a wide-field microscope with a 10 X air objective. Images were analyzed using ImageJ plugin OpenComet[19].

Statistical analysis and plotting

All statistical analysis was performed as indicated. Unless otherwise indicated, all replicates represent biological replicates. Test were carried out using GraphPad Prism version 8.3.0 (328) or R[20] using the ggpubr package[21]. Significance testing was performed using the tests indicated in the figures. For all plots, significance values are as follows: ns $p>0.05$; * $p<0.05$; ** $p<0.01$; *** $p<0.001$; **** $p<0.0001$. Box plots show first and third quartiles of the data as well as the median. In scenarios where multiple testing was considered, p-values were transformed into

FDR q-values by the qvalues package in R (Storey method)[22] unless otherwise indicated. Plots generated in R were generated using the ggplot[23], cowplot[24] and ggpubr packages. All R code, for data generation, analysis, and plotting is available upon request.

Supplemental References

1. McNerney, M. E., Brown, C. D., Wang, X., Bartom, E. T., Karmakar, S., Bandlamudi, C., *et al.* CUX1 is a haploinsufficient tumor suppressor gene on chromosome 7 frequently inactivated in acute myeloid leukemia. *Blood* **121**, 975–983 (2013).
2. Gundry, M. C., Brunetti, L., Lin, A., Mayle, A. E., Kitano, A., Wagner, D., *et al.* Highly efficient genome editing of murine and human hematopoietic progenitor cells by CRISPR/Cas9. *Cell Rep.* **17**, 1453–1461 (2016).
3. Brunetti, L., Gundry, M. C., Kitano, A., Nakada, D. & Goodell, M. A. Highly efficient gene disruption of murine and human hematopoietic progenitor cells by CRISPR/Cas9. *J. Vis. Exp.* **2018**, (2018).
4. Doench, J. G., Fusi, N., Sullender, M., Hegde, M., Vaimberg, E. W., Donovan, K. F., *et al.* Optimized sgRNA design to maximize activity and minimize off-target effects of CRISPR-Cas9. *Nat. Biotechnol.* **34**, 184–191 (2016).
5. An, N., Khan, S., Imgruet, M. K., Gurbuxani, S. K., Konecki, S. N., Burgess, M. R., *et al.* Gene dosage effect of CUX1 in a murine model disrupts HSC homeostasis and controls the severity and mortality of MDS. *Blood* **131**, 2682–2697 (2018).
6. Yuan, Z. F., Liu, C., Wang, H. P., Sun, R. X., Fu, Y., Zhang, J. F., *et al.* pParse: A method for accurate determination of monoisotopic peaks in high-resolution mass spectra. *Proteomics* **12**, 226–235 (2012).
7. MATLAB. 9.7.0.1190202 (R2019b). (2018).
8. Yuan, Z.-F., Sidoli, S., Marchione, D. M., Simithy, J., Janssen, K. A., Szurgot, M. R., *et al.* EpiProfile 2.0: A computational platform for processing Epi-proteomics mass spectrometry data. *J. Proteome Res.* **17**, 2533–2541 (2018).
9. Yuan, Z.-F., Lin, S., Molden, R. C., Cao, X.-J., Bhanu, N. V., Wang, X., *et al.* EpiProfile quantifies histone peptides with modifications by extracting retention time and intensity in high-resolution Mass Spectra. *Mol. Cell. Proteomics* **14**, 1696–1707 (2015).
10. Tyanova, S., Temu, T., Sinitcyn, P., Carlson, A., Hein, M. Y., Geiger, T., *et al.* The Perseus computational platform for comprehensive analysis of (prote)omics data. *Nat. Methods* **13**, 731–740 (2016).
11. Li, H. & Durbin, R. Fast and accurate short read alignment with Burrows-Wheeler

transform. *Bioinformatics* **25**, 1754–1760 (2009).

12. Li, H., Handsaker, B., Wysoker, A., Fennell, T., Ruan, J., Homer, N., *et al.* The Sequence Alignment/Map format and SAMtools. *Bioinforma. Appl. Note* **25**, 2078–2079 (2009).
13. Zhang, Y., Liu, T., Meyer, C. A., Eeckhoute, J., Johnson, D. S., Bernstein, B. E., *et al.* Model-based analysis of ChIP-Seq (MACS). *Genome Biol.* **9**, R137 (2008).
14. Stark, R. & Brown, G. DiffBind: Differential binding analysis of ChIP-Seq peak data. (2011).
15. Ramírez, F., Ryan, D. P., Bj¨, B., Grüning, B., Grüning, G., Bhardwaj, V., *et al.* deepTools2: a next generation web server for deep-sequencing data analysis. *Nucleic Acids Res.* **44**, W160-5 (2016).
16. Ovesný, M., Křížek, P., Borkovec, J., Švindrych, Z. & Hagen, G. M. ThunderSTORM: a comprehensive ImageJ plug-in for PALM and STORM data analysis and super-resolution imaging. *Bioinformatics* **30**, 2389–2390 (2014).
17. Dobin, A., Davis, C. A., Schlesinger, F., Drenkow, J., Zaleski, C., Jha, S., *et al.* Sequence analysis STAR: ultrafast universal RNA-seq aligner. **29**, 15–21 (2013).
18. Love, M. I., Huber, W. & Anders, S. Moderated estimation of fold change and dispersion for RNA-seq data with DESeq2. *Genome Biol.* **15**, 550 (2014).
19. Gyori, B. M., Venkatachalam, G., Thiagarajan, P. S., Hsu, D. & Clement, M. V. OpenComet: An automated tool for comet assay image analysis. *Redox Biol.* **2**, 457–465 (2014).
20. R Core Team. R: A Language and Environment for Statistical Computing. (2019).
21. Kassambara, A. ggpubr: 'ggplot2' Based Publication Ready Plots. (2020).
22. Storey, J. D., Bass, A. J., Dabney, A. & Robinson, D. qvalue: Q-value estimation for false discovery rate control. (2019).
23. Wickham, H. ggplot2: Elegant Graphics for Data Analysis. (2016).
24. Wilke, C. O. cowplot: Streamlined Plot Theme and Plot Annotations for 'ggplot2'. (2019).

Supplemental Information

Supplemental Table 1. EpiProfile Analysis following Irradiation

Supplemental Table 2. ChIP-seq and RNA-seq Sequencing Reads Table

ChIP-seq (H3K27me3)	**PF Clusters**	**Mapped reads (q30)**
K562 gHPRT H3K27me3 ChIP-seq Rep 1	4.71E+07	3.60E+07
K562 gCUX1 H3K27me3 ChIP-seq Rep1	3.95E+07	3.07E+07
K562 gHPRT H3K27me3 ChIP-seq Rep 2	4.09E+07	2.59E+07
K562 gCUX1 H3K27me3 ChIP-seq Rep2	3.72E+07	3.01E+07
RNA-seq on Murine HSCs	**PF Clusters**	**Mapped Reads (q30)**
Renilla_HSC_Rep1	7.76E+07	2.06E+07
Renilla_HSC_Rep2	7.19E+07	4.69E+07
Renilla_HSC_Rep3	5.57E+07	4.56E+07
Cux1-low HSC Rep1	7.07E+07	1.69E+07
Cux1-low HSC Rep2	6.48E+07	5.12E+07
Cux1-low HSC Rep3	6.10E+07	4.98E+07

Supplemental Table 3. Murine HSC RNA-seq

Supplemental Figure 1. CUX1 Recruits EHMT2 to Sites of DNA Damage

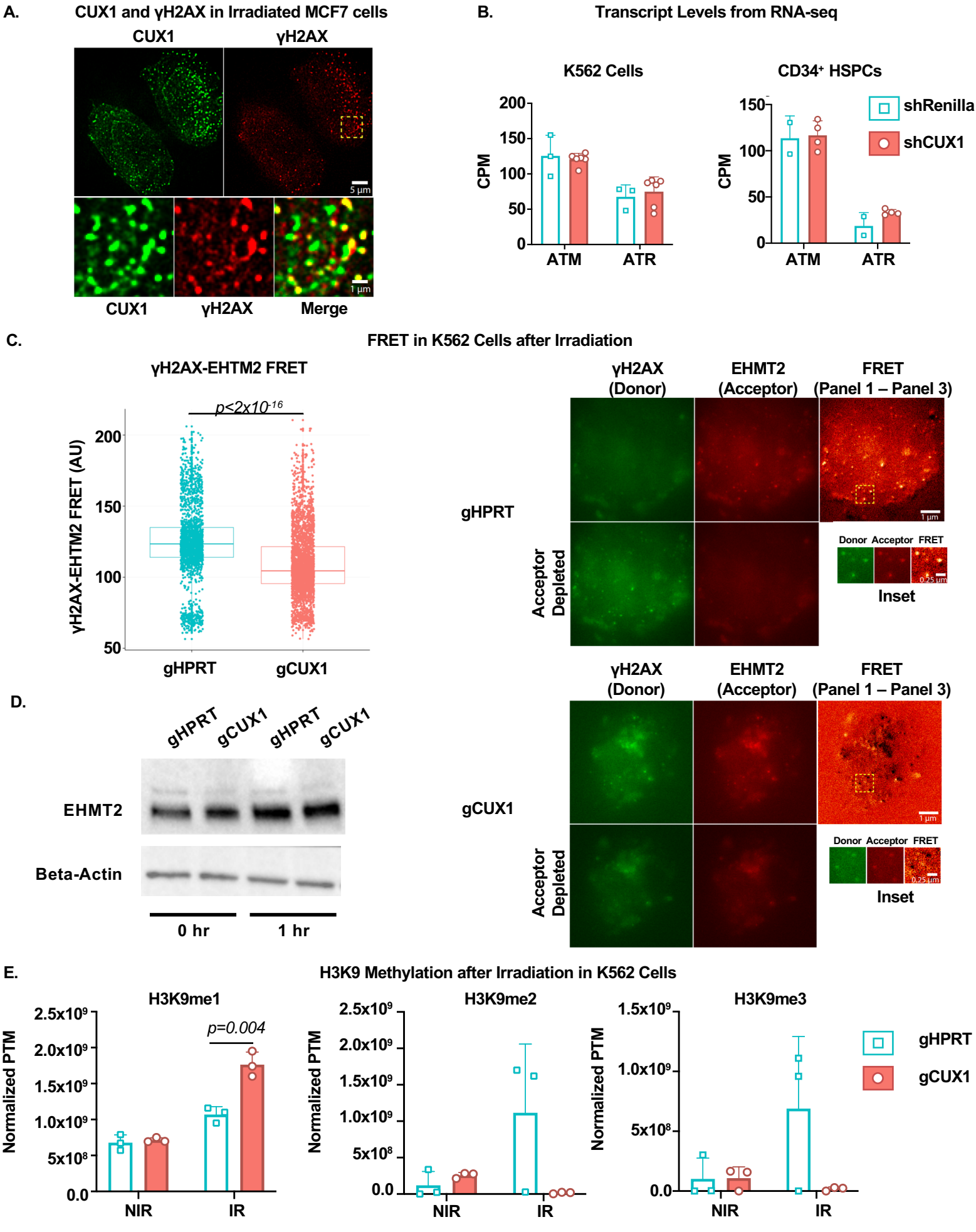

Supplemental Figure 1. CUX1 Recruits EHMT2 to Sites of DNA Damage

(A) Superresolution imaging of irradiated MCF7 cells showing CUX1 (green) and γH2AX (red). Colocalization of CUX1 with γH2AX is shown in yellow. Cells were fixed 1 hour after irradiation (6 Gy) and imaged on a Leica GSD imaging system (n=3).
(B) *ATM* and *ATR* transcripts measured by RNA-seq in shRenilla and shCUX1 cells in K562 cells (Arthur *et al.*, 2017) and human CD34 HSPCs (An *et al.*, 2018) (extracted from published RNA-seq data).
(C) GSD-FRET analysis of colocalization between γH2AX (donor) and EHMT2 (acceptor) in gHPRT and gCUX1 K562 cells one hour after irradiation (6 Gy). A representative image of the diminished FRET in gCUX1 cells is shown on the right panel (n=3).
(D) Representative immunoblot for EHMT2 protein in gHPRT and gCUX1 K562 cells (n=3).
(E) EpiProfile analysis of H3K9 methylation in irradiated and mock-irradiate gHPRT and gCUX1 cells. Histones were extracted 1 hour following irradiation (6 Gy). Three independent samples were collected.

Student *t* test, $p>0.05$; * $p<0.05$; ** $p<0.01$; *** $p<0.001$; **** $p<0.0001$.

Supplemental Figure 2. CUX1 Does Not Transcriptionally Regulate H3K27 Methyltransferases and Demethylases in Human Cells

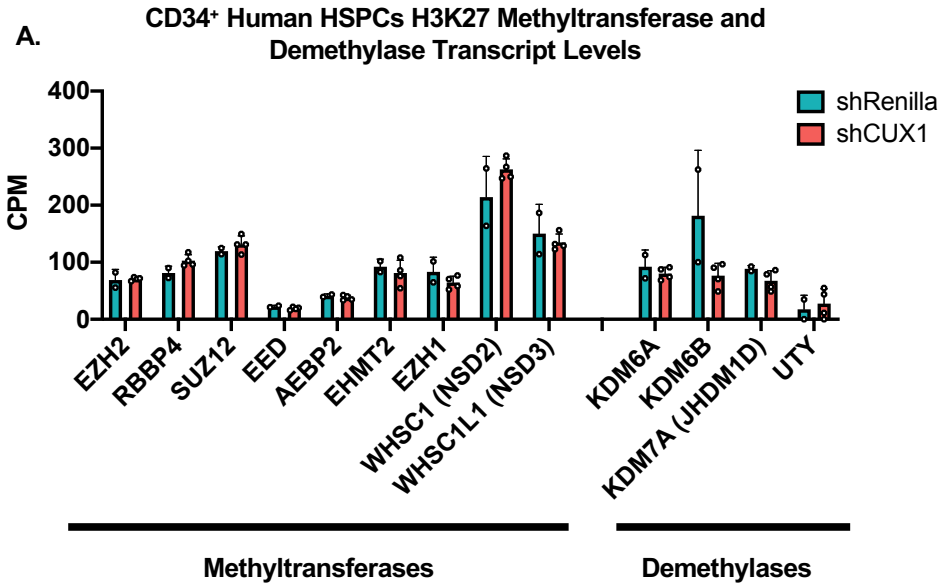

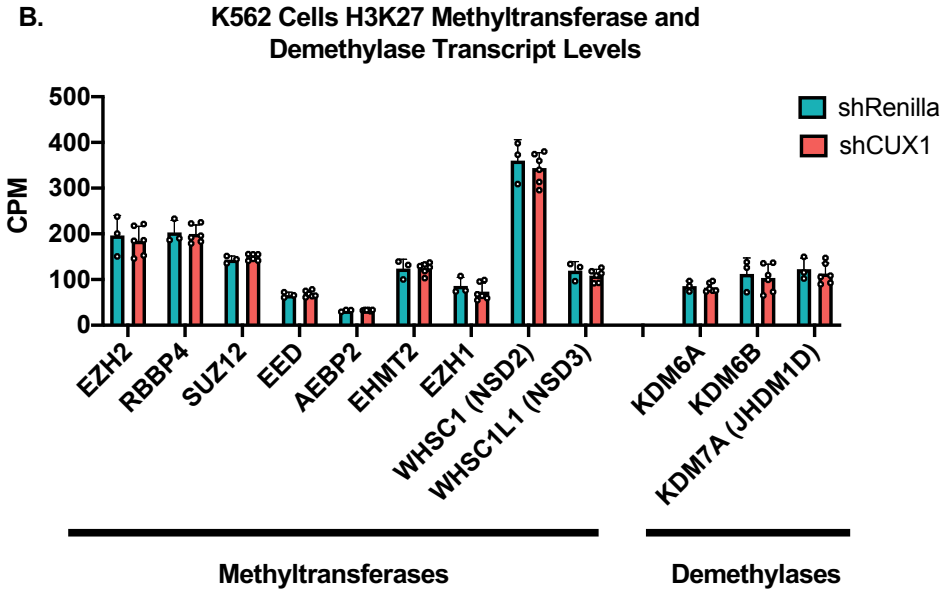

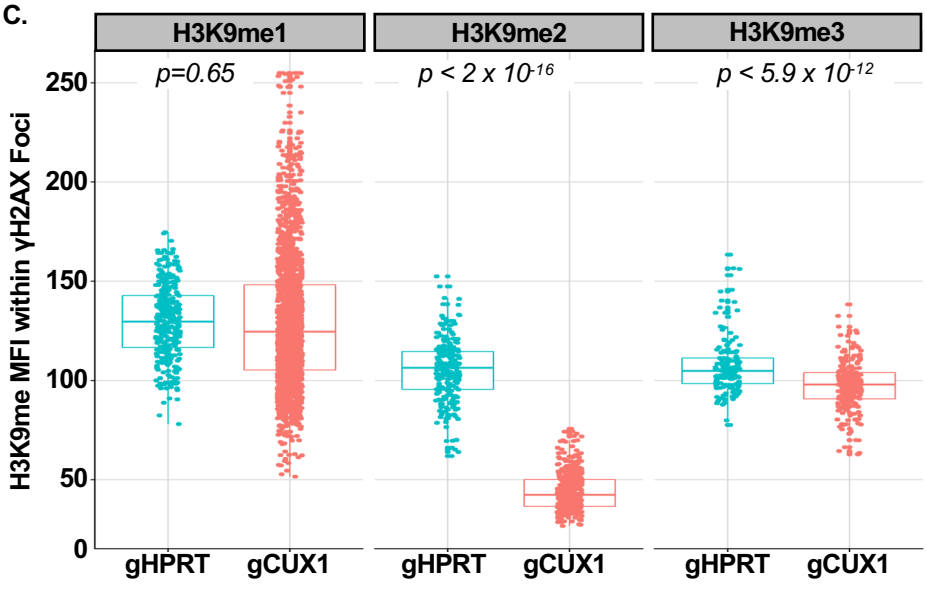

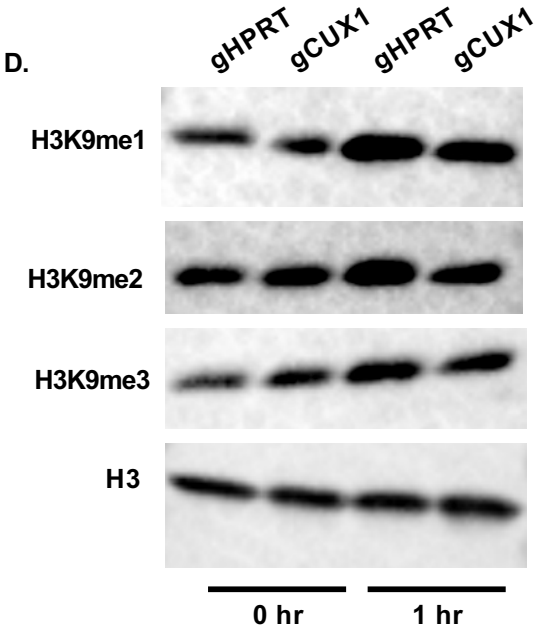

Supplemental Figure 2. CUX1 Does Not Transcriptionally Regulate H3K27 Methyltransferases and Demethylases in Human Cells

(A) Transcripts of H3K27 methyltransferases and demethylases in **(A)** human $CD34^+$ HSPCs (An *et al.*, 2018) and
(B) K562 cells (Arthur *et al.*, 2017) after CUX1 knockdown. (Extracted from previously published RNA-seq data).
(C) Cells were imaged for antibodies targeting γH2AX and H3K9 methylation 1 hour following irradiation. H3K9me1/2/3 MFI was quantified within each γH2AX foci (n=2).
(D) Representative immunoblot for H3K9me1, H3K9me2 and H3K9me3 in gHPRT and gCUX1 K562 cells (n=3).

Supplemental Figure 3. CUX1 Does Not Transcriptionally Regulate H3K27 Methyltransferases and Demethylases In Murine HSCs

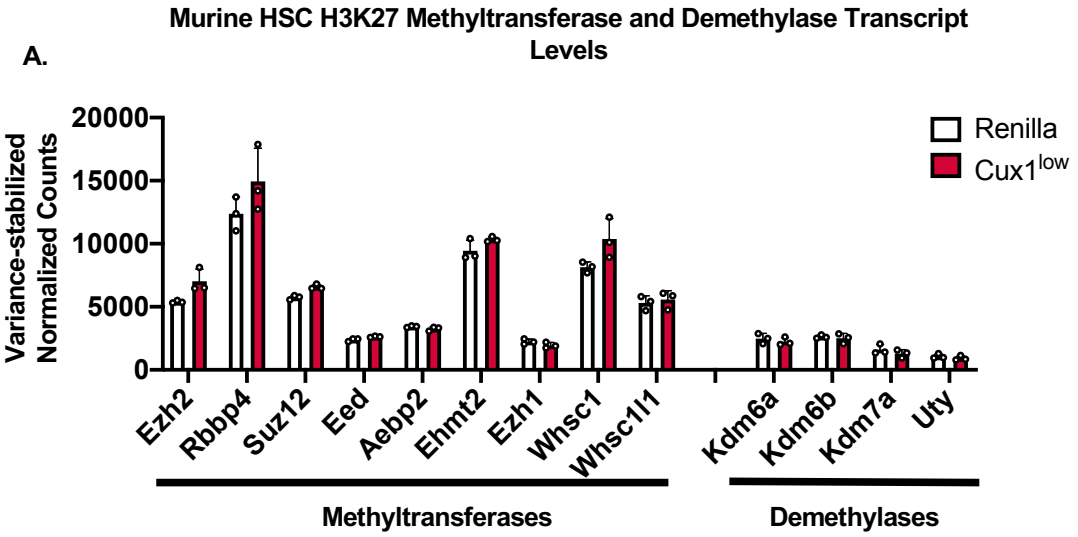

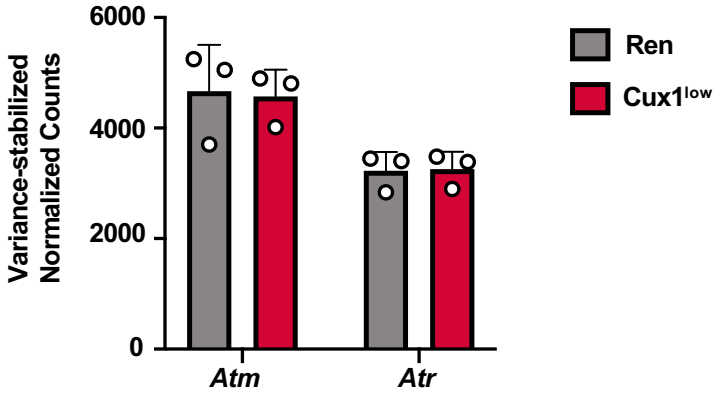

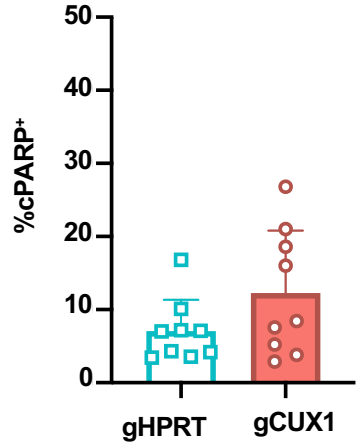

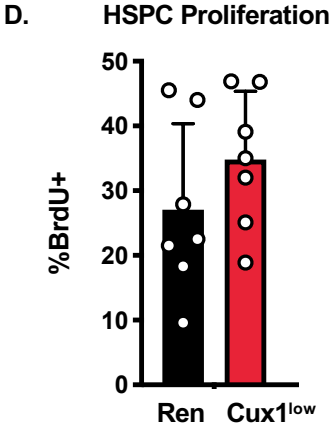

Supplemental Figure 3. CUX1 Does Not Transcriptionally Regulate H3K27 Methyltransferases and Demethylases in Murine HSCs

(A) Expression of H3K27 methyltransferases and demethylases in murine HSCs (lineage$^-$/cKit$^+$/Sca1$^+$/CD135$^-$) from RNA-seq data (n=3).
(B) *Atm* and *Atr* transcripts by RNA-seq from sorted murine HSCs
(C) Samples were collected as in Figure 4F, and cPARP$^+$ cells were gated to measure apoptosis (n=3). Three biological replicates are shown.
(D) Proliferation was measured in Ren and Cux1^{low}. Mice were treated with doxycycline for 16 days. BrdU was administered I.P. BrdU+ cells were measured by flow cytometry 12 hours after BrdU injection in the bone marrow HPSC population (Lin$^-$). The mean ± SD and Student t test p value is shown.

Supplemental Figure 4. Cux1-Deficient Mice Develop a Therapy-Related Myeloid Neoplasm After Alkylator Chemotherapy

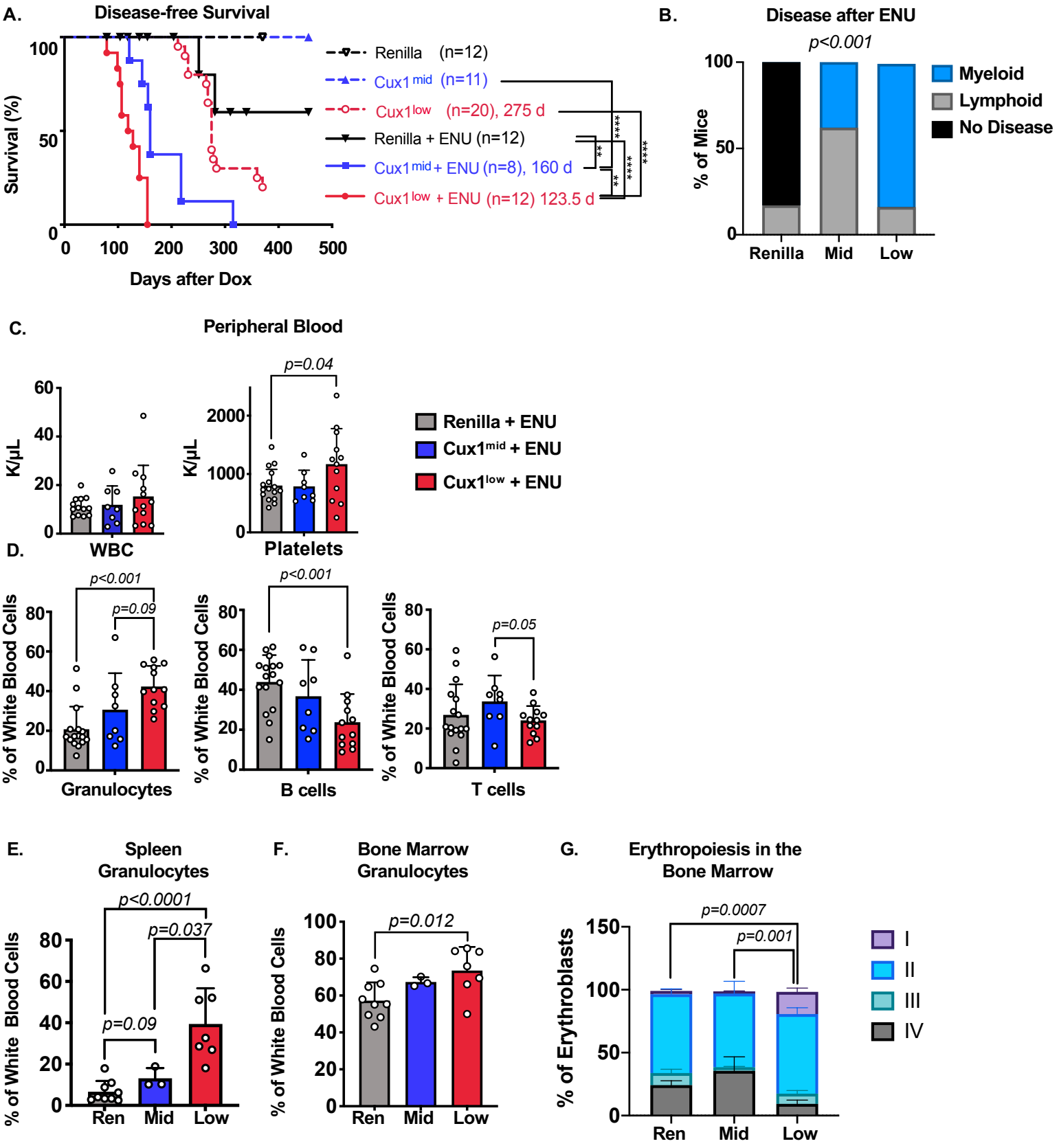

Supplemental Figure 4. Cux1-Deficient Mice Develop a Therapy-Related Myeloid Neoplasm After Alkylator Chemotherapy

(A) Kaplan-Meier plot showing decreased survival (all-cause) for $Cux1^{mid}$ (n=8) and $Cux1^{low}$ (n=12) mice treated with ENU compared to Ren mice treated with ENU (n=12). Median survival data shown for Ren, $Cux1^{mid}$ and $Cux1^{low}$ mice without the addition of ENU (dashed lines) was previously published (An *et al.*, 2018). Log-rank test *p <.05, **p .<01, ***p < .001

(B) Histologic classification of diseases arising in the mice. 2/12 Renilla mice develop lymphoid disease; 3/8 $Cux1^{mid}$ mice develop myeloid and 5/8 develop lymphoid disease; 10/12 $Cux1^{low}$ mice develop myeloid and 2/12 develop lymphoid disease. Chi-square test.

(C) Complete blood counts of the peripheral blood of Ren, $Cux1^{mid}$ and $Cux1^{low}$ mice at autopsy. White blood cell counts (WBC) platelet counts are shown. The mean ± SD and Student *t* test p values are shown.

(D) Flow cytometry analysis of the peripheral blood at autopsy for granulocytes ($Gr1^+/CD11b^+$), B cells ($B220^+$) and T cells ($CD3e^+$). The mean ± SD and Student *t* test p values are shown.

(E) Flow cytometry of the (E) spleen and

(F) bone marrow at autopsy. Granulocytes are quantified as a percentage of white blood cells ($CD45^+$) in mice with non-lymphoid disease. The mean ± SD and Student *t* test p values are shown.

(G) RI-RIV erythroid precursor populations in the bone marrow. Populations are quantified as percentage of erythroblasts ($CD71^+$ or $Ter119^+$) in mice with non-lymphoid disease. An ordinary two-way ANOVA was performed, p values are shown.

Supplemental Figure 5. Cux1-Deficient Mice Show an Immature Erythroid Expansion into Non-Hematopoietic Organs

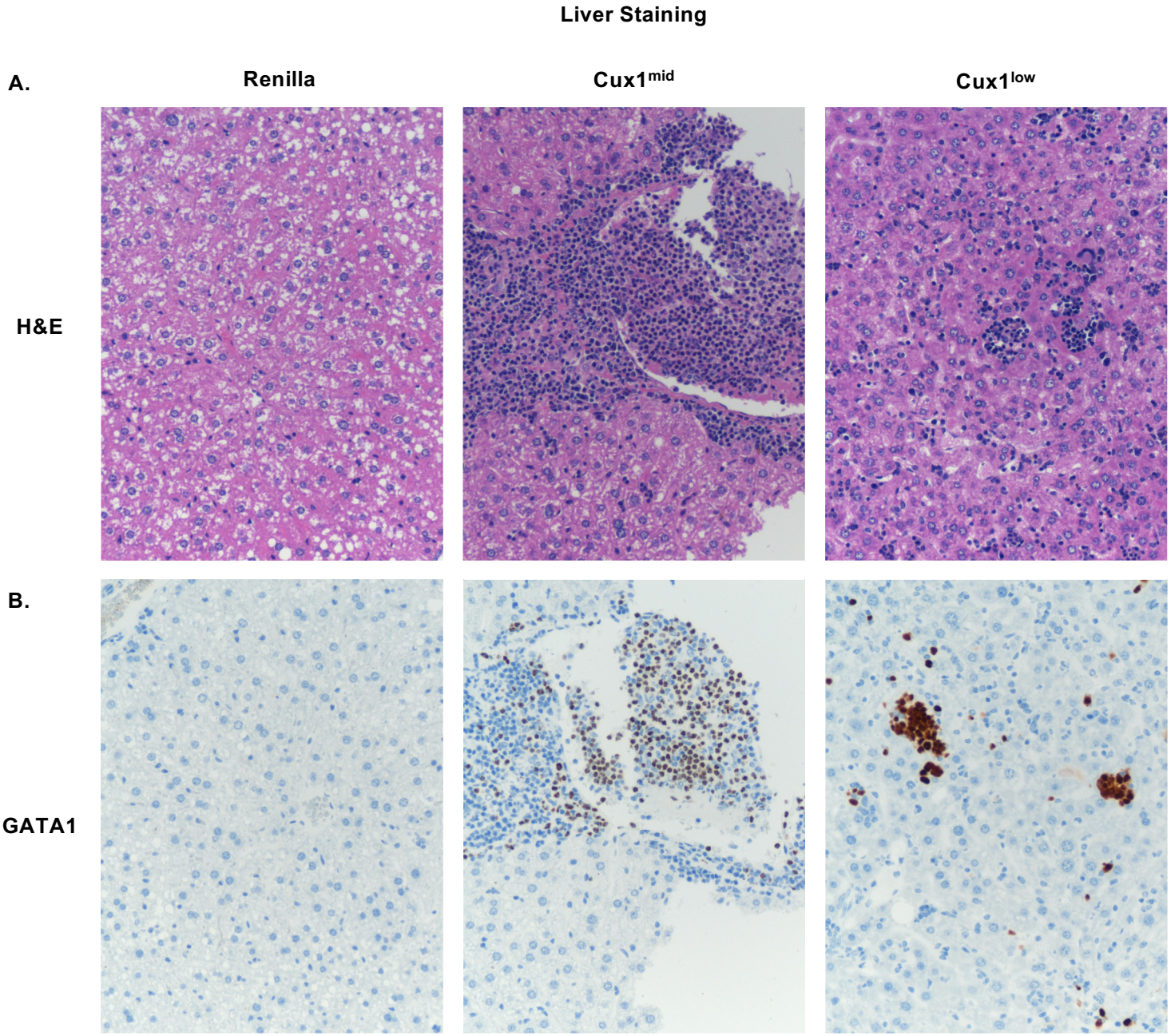

Supplemental Figure 5. Cux1-Deficient Mice Show an Immature Erythroid Expansion into Non-Hematopoietic Organs

(A) Representative images of Renilla, Cux1^{mid} and Cux1^{low} liver H&E stains.
(B) Representative images of Renilla, Cux1^{mid} and Cux1^{low} liver stained for GATA1